

Second Harmonic Imaging in Random Media

Wei Li

Louisiana State University

Joint work with Liliana Borcea, Alexander Mamonov and John Schotland
Inverse Problems, 2017(33), 065004

May 21, 2018

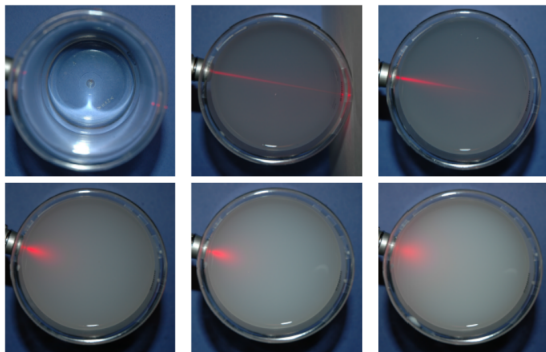
The imaging problem

- Goal: **Locate** targets in a **scattering medium**.
- Scattering media has many unknown inhomogeneities, time reversal would not work (human tissues, the atmosphere, construction materials, etc).
- Model the media as **realizations of a random process**. Wave equations contain random coefficients.
- Each sample is one realization. Predictions has to be **statistically stable**, characterized by a big **SNR** = $\frac{\mathbb{E}[\cdot]}{\sqrt{\text{Var}[\cdot]}}$.

Length scales of a scattering medium

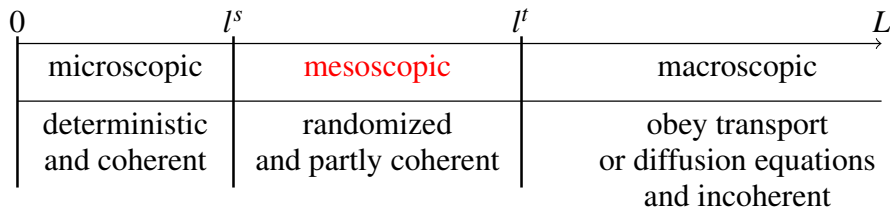
- **The scattering mean free path** / mean free path l^s : the average distance between two scattering events of a photon.
- **The transport mean free path** / transport length l^t : the average distance after which the travel direction of a photon is randomized (the wave does not have a well defined propagation direction).
- **Propagation distance L**: the size of the medium.

Scattering regimes



Scattering regimes for different scattering media (fixed L).
Image credit: John Schotland (and daughter).

Scattering regimes and imaging methods



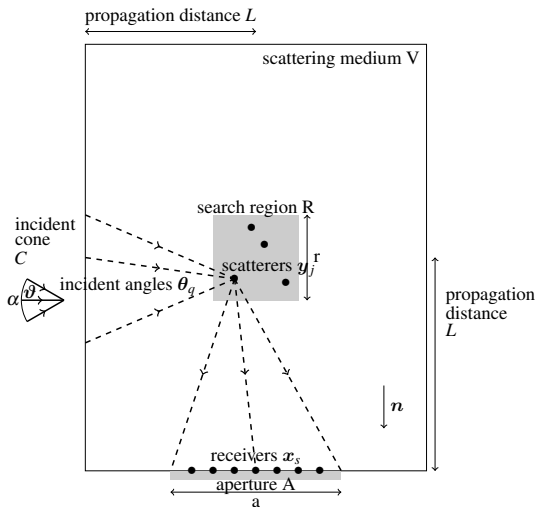
Scattering regimes for L 's (fixed medium).

Imaging methods for mesoscopic problems

- **Incoherent** methods (**intensity** is measured):
 - confocal microscopy
 - optical projection tomography
 - single-scattering optical tomography
- **Coherent** methods (both **phase and intensity** are measured):
 - optical coherence microscopy
 - interferometric synthetic aperture microscopy
 - **coherent interferometry (CINT)**
- Works on imaging of nonlinear scatterers in the mesoscopic regime
 - experimental: Brown-McKee-diTomaso-Pluen-Boucher-Jain '03, SeedHsieh-Grange-Pu-Psaltis '09
 - theoretical: Habib-Garnier-Millien '14
- Works on CINT Borcea-Papanicolaou-Tsogka '05, '06, '07, Borcea-Garnier-Papanicolaou '11

Set up of imaging

- Scalar wave equation
- 2D
- Linear medium (η)
- Second-order nonlinear scatterers (η_1 and η_2)
- Illumination fields: plane waves ($k = \omega/c$ and θ_q)
- Second-harmonic generation: fields at ω and 2ω are present.



Wave equations

- Incident field $u_{1,0}^{(i)}(x; \theta_q) = e^{ik\theta_q \cdot x}$:

$$\Delta u_{1,0}^{(i)}(x; \theta) + k^2 u_{1,0}^{(i)}(x; \theta) = 0.$$

- $u_1(x; \theta)$ and $u_2(x; \theta)$: the fields at frequency ω and 2ω .
- Wave equations:

$$\begin{aligned} \Delta u_1(x; \theta) + k^2 [1 + 4\pi \eta(x)] u_1(x; \theta) \\ = -4\pi k^2 [\eta_1(x) u_1(x; \theta) + 2\eta_2(x) u_2(x; \theta) u_1^*(x; \theta)] , \end{aligned}$$

$$\begin{aligned} \Delta u_2(x; \theta) + (2k)^2 [1 + 4\pi \eta(x)] u_2(x; \theta) \\ = -4\pi (2k)^2 [\eta_1(x) u_2(x; \theta) + \eta_{2(x)} u_1^2(x; \theta)] . \end{aligned}$$

Measured fields and data

- Measured fields at the receivers x_s

$$u_1(x_s, \boldsymbol{\theta}_q), u_2(x_s, \boldsymbol{\theta}_q), \quad s = 1, \dots, N_x, \quad q = 1, \dots, N_\theta.$$

- Data:

$$d_1(x_s, \boldsymbol{\theta}_q) = u_1(x_s; \boldsymbol{\theta}_q) - u_{1,0}^{(i)}(x_s; \boldsymbol{\theta}_q),$$
$$d_2(x_s, \boldsymbol{\theta}_q) = u_2(x_s; \boldsymbol{\theta}_q).$$

Analysis: ideas and results

- The forward model
 - Kinematics: The propagation of the wave is in the scaling regime of **geometric optics with randomized phases**.
 - Dynamics: The scattering off the targets are approximated by **the Born approximation** (waves are scattered once by the scatterers).
- The reconstruction
 - The migration imaging functions are superpositions of **the backpropagated data**.
 - The coherent-interferometry (**CINT**) imaging functions are superpositions of the backpropagated **crosscorrelations** of the data.
- The performance
 - CINT is more trustworthy (**stable**) than migration because CINT mitigates the random phases (at the expense of resolution).
 - The image of the nonlinear η_2 has **no spurious peaks**.

Forward model of the data

- Born approximations:

$$u_1(x; \theta) \approx u_1^{(i)}(x; \theta) + k^2 \int dy \eta_1(y) G(x, y; \omega) u_1^{(i)}(y; \theta),$$

$$u_2(x; \theta) \approx (2k)^2 \int dy \eta_2(y) G(x, y; 2\omega) [u_1^{(i)}(y; \theta)]^2,$$

where G is the Green function **in the random medium**:

$$\Delta G(x, y; \omega) + k^2 [1 + 4\pi\eta(x)] G(x, y; \omega) = -4\pi i \delta(x),$$

and $u_1^{(i)}$ **the randomized** incident field:

$$\Delta u_1^{(i)}(x; \theta) + k^2 [1 + 4\pi\eta(x)] u_1^{(i)}(x; \theta) = 0.$$

Migration in optically thin media

- The standard Migration imaging function (whose **peaks** are the estimated locations of the scatterers) is

$$I_j^M(y^R) = \sum_{s=1}^{N_x} \sum_{q=1}^{N_\theta} G_0^*(y^R, x_s; j\omega) e^{-ijk\theta_q \cdot y^R} d_j(x_s, \theta_q) =: (jk)^2 \int_V dy \eta_j(y) K_j^M(y^R, y).$$

$$G_0(x, y; \omega) = \frac{e^{ik|x-y|}}{|x-y|}.$$

- If the medium is **optically thin**:

$$u_1^{(i)}(x_s; \theta_q) \approx u_{1,0}^{(i)}(x_s; \theta_q) \quad \text{and} \quad G(x_s, y; j\omega) \approx G_0(x_s, y; j\omega),$$

then the **point spread function** of the imaging function is

$$K_j^M(y^R) = \sum_{s=1}^{N_x} \sum_{q=1}^{N_\theta} G_0^*(y^R, x_s; j\omega) e^{-ijk\theta_q \cdot y^R} G_0(x_s, y; j\omega) e^{ijk\theta_q \cdot y}.$$

- It peaks at $y^R \approx y$ due to constructive superposition with resolution $\lambda L / (ja)$.
- It breaks down when the cumulative scattering is not negligible.

Model of the scattering background

- Suppose that the random medium consists of small, mean zero fluctuations which lacks long range correlations and has an integrable autocorrelation function:

$$4\pi\eta(x) = \sigma\mu\left(\frac{x}{l}\right).$$

- μ is a bounded, mean zero and stationary random process, which lacks long range correlation.
- l is **the correlation length**, the spatial scale over which the autocorrelation decays.
- σ is **the amplitude** of the fluctuations.
- For convenience (elementary formulas), suppose the autocorrelation takes the form

$$\mathbb{E}[\mu(h)\mu(0)] = e^{-\frac{|h|^2}{2}}.$$

Geometrical optics in random media

- Random geometrical optics wave propagation model

$$\lambda \ll l \ll L,$$

$$\sigma \ll (l/L)^{3/2}, \quad \sigma \ll \sqrt{\lambda l}/L.$$

the waves propagate along straight lines, the variance of the amplitude of the Green function is negligible.

Geometrical optics in random media

- The Green function is

$$G(x, y; j\omega) = G_0(x, y; j\omega)e^{ijkv(x,y)}, \quad \text{for } x \in A \text{ and } y \in R,$$

where

$$v(x, y) = \frac{\sigma|x-y|}{2} \int_0^1 dt \mu \left(\frac{(1-t)y}{l} + \frac{tx}{l} \right).$$

- The randomized incident wave is

$$u_1^{(i)}(x; \theta) = e^{ik\theta \cdot x + ik\gamma(x, \theta)}, \quad \text{for } x \in A \text{ and } \theta \in C,$$

where

$$\gamma(x, \theta) = \frac{\sigma|x-x^{(i)}(\theta)|}{2} \int_0^1 dt \mu \left(\frac{(1-t)x}{l} + \frac{tx^{(i)}(\theta)}{l} \right).$$

- $v(x, y)$ and $\gamma(x, \theta)$ are approximately Gaussian.

Randomization of the waves

- Large wavefront distortions

$$\sigma \gg \frac{\lambda}{\sqrt{lL}}.$$

consistent when $l \gg \sqrt{\lambda L}$.

- Paraxial regime

$$a \ll (\lambda L^3)^{1/4} \ll L,$$

and

$$r \ll \frac{\lambda L^2}{a^2} \ll a.$$

Randomization of the waves

- The expectation of the Green function is

$$\begin{aligned}\mathbb{E}[G(x, y; j\omega)] &= G_0(x, y; j\omega)\mathbb{E}[\exp[ij\mathbf{k}\mathbf{v}(x, y)]] \\ &\approx G_0(x, y; j\omega)\exp\left[-\frac{(jk)^2\mathbb{E}[\mathbf{v}^2(x, y)]}{2}\right] \\ &= G_0(x, y; j\omega)\exp\left[-\frac{|x-y|}{S_j}\right],\end{aligned}$$

where S_j are the mean scattering free paths:

$$S_j = \frac{8}{\sqrt{2\pi}\sigma^2(jk)^2l} \ll L.$$

- The expectation of the norm square of the Green function is

$$\mathbb{E}[|G(x, y)|^2] = \mathbb{E}[|G_0(x, y)|^2].$$

- Thus the SNR is exponentially small for $|x-y| \sim L$.

Migration is unstable

- The signal-to-noise ratio (SNR) of the Migration imaging functions are

$$SNR(I_j^M(y^R)) := \frac{\mathbb{E}[|I_j^M(y^R)|^2]}{SD[I_j^M(y^R)]} \propto \exp\left[-\frac{|x-y|}{S_j}\right].$$

This is exponentially small near the location of the scatterers.

- It fails to focus or the peaks change unpredictably with the realizations of the random medium.
- This is caused by the large random phases of the Green function (and the incident field).

CINT imaging functions

The CINT imaging function is

$$I_j^{CINT}(y^R)(\bar{x}_s, \bar{\theta}_q, y^R) = \sum_{\tilde{s}=1}^{\tilde{N}_x} \sum_{\tilde{q}=1}^{\tilde{N}_\theta} \Phi\left(\frac{\tilde{x}_{\tilde{s}}}{X_j}\right) \Phi\left(\frac{\tilde{\theta}_{\tilde{q}}}{\Theta_j}\right) \\ \times b_j\left(\bar{x}_s + \frac{\tilde{x}_{\tilde{s}}}{2}, \bar{\theta}_q + \frac{\tilde{\theta}_{\tilde{q}}}{2}, y^R\right) b_j^*\left(\bar{x}_s - \frac{\tilde{x}_{\tilde{s}}}{2}, \bar{\theta}_q - \frac{\tilde{\theta}_{\tilde{q}}}{2}, y^R\right),$$

which uses **local correlations to eliminate random phases and extract deterministic phases**. Here Φ is a window function,

$$b_j(x_s, \theta_q, y^R) = d_j(x_s, \theta_q) G_0^*(y^R, x_s; j\omega) e^{-ijk\theta_q y^R},$$

the center-offsets coordinates for the receivers are

$$\bar{x}_{ss'} = (x_s + x_{s'})/2, \quad \tilde{x}_{ss'} = x_s - x_{s'}, \quad s, s' = 1, \dots, N_x,$$

and those for the incident directions are

$$\bar{\theta}_{qq'} = (\theta_q + \theta_{q'})/2, \quad \tilde{\theta}_{qq'} = \theta_q - \theta_{q'}, \quad q, q' = 1, \dots, N_\theta.$$

Decorrelation of the waves and choice of window widths

- The second moment of the Green function is

$$\mathbb{E} [G(x, y; j\omega) G^*(x', y; j\omega)] \approx \frac{1}{L^2} \exp \left[ijk \left(L + \frac{|x_{\perp} - y_{\perp}|^2}{2L} \right) - \frac{|x'_{\perp} - x_{\perp}|^2}{2X_{d,j}^2} \right],$$

where

$$X_{d,j} = l \sqrt{\frac{3S_j}{2L}} = O \left(\frac{\lambda \sqrt{l}}{\sigma \sqrt{L}} \right) \ll l.$$

- The second moment of the randomized incident wave is

$$\mathbb{E} \left[u_1^d(x, \theta) \overline{u_1^d(x', \theta')} \right] \approx e^{ik(x \cdot \theta - x' \cdot \theta') - \frac{3|P_{\tilde{\theta}} \tilde{x}|^2 - 3|x-x^{(i)}(\theta)|\tilde{x} \cdot P_{\tilde{\theta}} \tilde{\theta} + |x-x^{(i)}(\theta)|^2 |P_{\tilde{\theta}} \tilde{\theta}|^2}{2X_{d,1}^2}},$$

where $\tilde{x} = x - x'$, $\tilde{\theta} = \theta - \theta'$.

Decorrelation of the waves and choice of window widths

- The second moments of the waves impinging on the scatterer at y are

$$\mathbb{E} \left[u_1^d(y, \theta) \overline{u_1^d(y, \theta')} \right] \approx e^{iky \cdot \tilde{\theta} - \frac{|P_{\vartheta} \tilde{\theta}|^2}{2\Theta_d^2}},$$

where

$$\Theta_d = \frac{X_{d,1}}{|y - y^{(i)}(\vartheta)|} \ll \frac{l}{L}.$$

- The incident waves and the scatterers waves decorrelate:

$$a \gg (\lambda L^2)^{1/3}.$$

- These second moments are exponentially small over receiver location offsets comparable to the decorrelation length $X_{d,j}$, or over incident angle offsets comparable to the decorrelation angle Θ_d .

Choose $X \approx X_j$ and $\Theta_j \approx \Theta_d/j$.

Stability of CINT

- CINT is statistically stable when

$$a \gg l.$$

- Note that all the above scaling constraints are consistent

$$\lambda \ll \sqrt{\lambda L} \ll l \ll (\lambda L^2)^{1/3} \ll a \ll (\lambda L^3)^{1/4} \ll L,$$

$$\frac{\lambda}{\sqrt{lL}} \ll \sigma \ll \frac{\sqrt{\lambda l}}{L}.$$

The CINT image of the quadratic susceptibility

- The expectation of the CINT image of η_2 is

$$\mathbb{E} [I_2^{CINT}(y^R)] \approx \frac{(2\pi)^3}{2} \left(4k^2 \langle \eta_2 \rangle^2 \alpha \Theta_e \frac{aX_e}{L^2} \right)^2 \\ \times \exp \left[-\frac{1}{2} \left(\frac{2kX_e |y_{\perp} - y_{\perp}^R|}{L} \right)^2 - \frac{1}{2} (2k\Theta_e |P_{\vartheta}(y - y^R)|)^2 \right].$$

- The Variance of the CINT image of η_2 is $(l/a)^2 \mathbb{E} [I_2^{CINT}(y^R)]^2$
- The **SNR** of the imaging function evaluated at the scatterer location is of the order $a/l \gg 1$.
- The **resolution** is $\frac{L\lambda}{X_e}$, which is worse than the resolution of the migration images in homogeneous media $\frac{L\lambda}{2a}$.
- The peak of the CINT image can be observed in the **search region R with linear size r** since $\frac{\lambda L/X_e}{\lambda L^2/a^2} \ll 1$.

The CINT image of η_1

- The CINT image of η_1 has **big spurious peaks near the receiver array**.
- Recall that

$$d_1(x_s, \theta_q) = u_1(x_s; \theta_q) - u_{1,0}^{(i)}(x_s; \theta_q),$$
$$d_2(x_s, \theta_q) = u_2(x_s; \theta_q).$$

- It's caused by the uncompensated distorted incident wave in the data.
- The image of η_2 does not suffer from this problem.

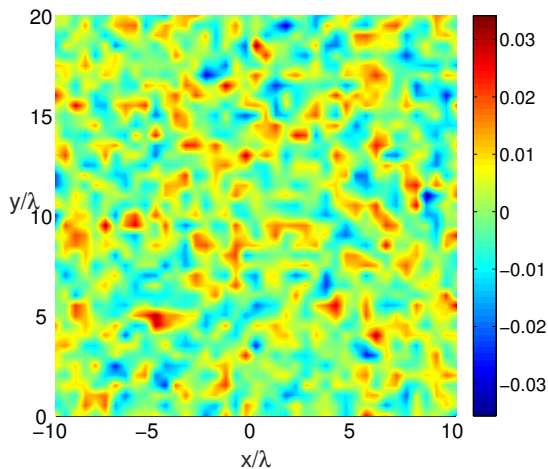
Numerics: another scaling regime

- The scalings for the numerics is **different from geometric optics in random media**:

$$L = 20\lambda, \quad l = 0.3\lambda, \quad a = 20\lambda, \quad \sigma = 0.01 * 4\pi,$$
$$X_1/2 = X_2 = 7\lambda, \quad \Theta = \frac{\pi}{5}.$$

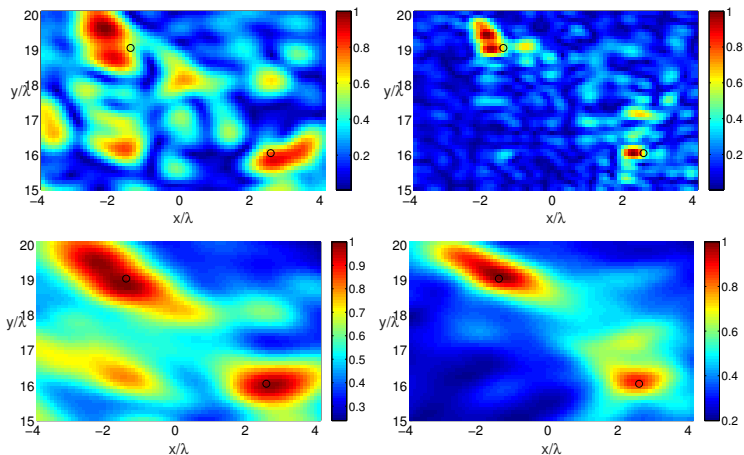
- All the above results **hold qualitatively**.

One realization of the random medium



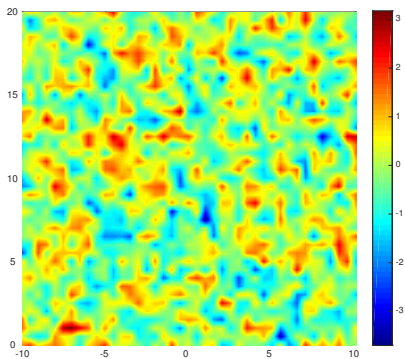
First realization of η .

Images



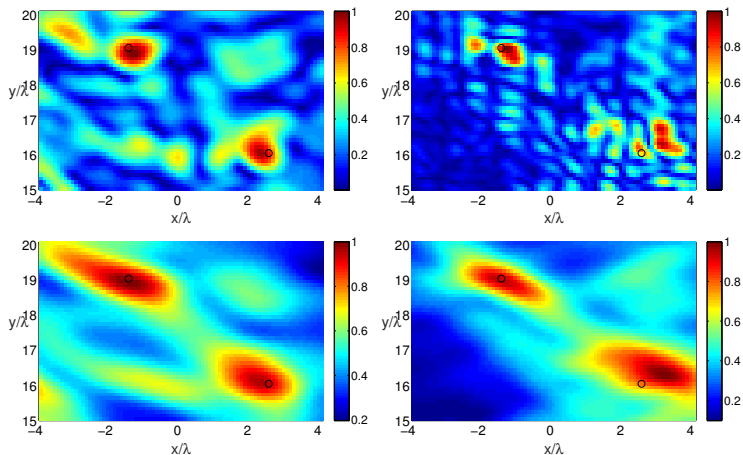
The Migration (top) and CINT (bottom) images of η_1 (left) and η_2 (right).

Another realization of the random medium



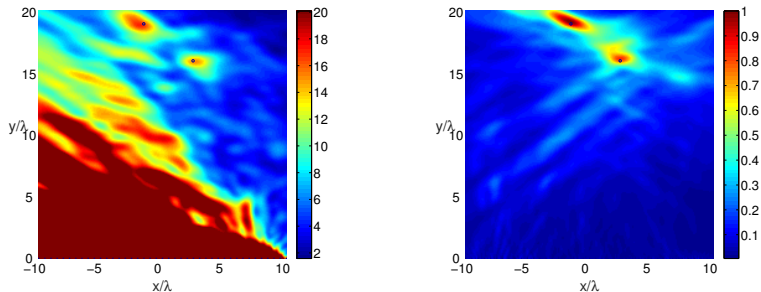
Another realization of η .

Images



The Migration (top) and CINT (bottom) images of η_1 (left) and η_2 (right).

Numerics



The CINT images of η_1 (left, rescaled) and η_2 (right) in the entire domain.

Thank you!